Title;
Causal Network Analysis of Heavy Snowfall Systems: North American Great Lakes vs. Sea of Japan Coast

Author Hiroshi MATSUDA
Kokusai Kogyou Co., Ltd.,
2-24-1, Harumi-cho, Fuchu-shi, Tokyo 183-0057
hiroshi_matsuda@kk-grp.jp
ORCID:https://orcid.org/0009-0005-5537-3749

Causal Network Analysis of Heavy Snowfall Systems: North American Great Lakes vs. Sea of Japan Coast

Hiroshi MATSUDA[1*] and Shin'ichi HOMMA[1]
[1] Kokusai Kogyou Co., Ltd.,

2-24-1, Harumi-cho, Fuchu-shi, Tokyo 183-0057
*Corresponding author: hiroshi_matsuda@kk-grp.jp

*ORCID: https://orcid.org/0009-0005-5537-3749

Abstract

This study conducts a hydro-climatic comparative analysis of two regions prone to heavy urban snowfall: the eastern shores of the North American Great Lakes (Lake-Effect Snow: LES) and the coast of the Sea of Japan (Sea-Effect Snow: SES). We introduce a quantitative metric—water vapor conversion efficiency (η = snowfall amount/PW)—and apply a data-driven causal discovery framework (DirectLiNGAM). Building upon challenges identified in previous studies (e.g., Fujisaki-Manome et al., 2022; West et al., 2019; Steenburgh and Nakai, 2020), we present the following five new findings:

- **(1)** Mathematical modeling of a discontinuous "risk jump" ($\mathcal{J}_{\text{risk}}$) using the Heaviside step functions.
- **(2)** Construction of causal Directed Acyclic Graphs (DAGs) that distinguish between physical topological differences.
- **(3)** Characterization of properties through non-stationary Generalized Extreme Value (GEV) distribution analysis spanning over 80 years (confirming a Weibull-type distribution with an upper bound ($\xi = -0.12 < 0$) for the Great Lakes and a heavy-tailed Fréchet-type distribution ($\xi = +0.18 > 0$) for Japan).
- **(4)** Identification of a memory effect regarding water vapor accumulation over 1–2 days (lag 1–2: $r = 0.78$).
- **(5)** Quantification of differences in amplification effects attributable to topographic conditions, Japan's steep mountain ranges (elevations of 2,000–3,000 m) versus the US's gentle plateaus (elevations of 300–500 m).

We report on these five results.

Keywords: Causal Network Analysis; Heavy Snowfall Systems; North American Great Lakes; Sea of Japan Coast;DAGs; Direct LiNGAM; Non-stationary GEV; maximam snowfall; Lake-Effect Snow;Sea-Effect Snow

1 Introduction

Record-breaking heavy snowfall poses significant risks to social infrastructure—such as transportation and power grids—and raises safety concerns regarding avalanches in mountainous areas. This paper compares and examines the mechanisms behind heavy snowfall in two regions of the world where such events frequently occur in urban areas.

"Lake-Effect Snow" (LES) in the Great Lakes region of the United States and "Sea-Effect Snow" (SES) along the Sea of Japan coast share a common thermodynamic mechanism: cold, dry polar air masses acquire sensible and latent heat as they pass over relatively warm water surfaces (fetch).

Along the Sea of Japan coast—such as in Takada (91 cm/day) and Tokamachi (101 cm/day)—a phenomenon is observed wherein snowfall efficiency increases sharply and non-linearly once temperature and humidity exceed certain thresholds; we define this phenomenon as a "Risk Jump." In contrast, studies on the Great Lakes region (e.g., Buffalo, at 71.1 cm/day) offer qualitative explanations regarding contrasts in cloud scale and topography—such as the fact that snow clouds over the Great Lakes are shallower (cloud-top heights < 2–3 km) than those over the Sea of Japan, and that the terrain inland (e.g., the Tug Hill Plateau) has an elevation of only 300–500 m [2]. Other studies qualitatively describe thermodynamic processes wherein lake ice cover during mid-winter limits the fetch, thereby reducing or cutting off heat and water vapor fluxes (evaporation) from the water surface and suppressing or altering the occurrence and intensity of lake-effect snow [3]. Previous studies [1–3] have relied primarily on qualitative conceptual models or instantaneous data (snapshots) from satellite observations, without analyzing causal networks or the probabilistic structure of non-stationary extreme events.

In this paper, we analyzed the hydro-thermodynamic mechanisms governing snowfall in these two distinct regions by utilizing synchronized observational data spanning multiple winter seasons (2020/21 and 2022/23), 84 years of daily snowfall data (1940–2023), two-dimensional response surfaces, time-lagged cross-correlation, and DirectLiNGAM—a causal discovery method.

2 Data and Methodology

2.1 Observational and Reanalysis Datasets

The datasets utilized in this study are summarized in Table 1.

Table 1: Overview of observational and reanalysis datasets used in this study.

Region	Station / Grid	Topographic Features / Elev.	Source	Period	Key Variables
Sea of Japan (Japan)	**Takada** (Niigata)	Coastal Foothills (13m) / Deep Mode	JMA AMeDAS	1886–2023	Daily Snowfall S, Snow Depth, Temp
	Toyama (Toyama)	Coastal Plain (9m) / Direct JPCZ	JMA AMeDAS	1939–2023	Daily Snowfall S, Snow Depth, Temp
	Sapporo (Hokkaido)	Ishikari Plain (17m) / Shallow Mode	JMA AMeDAS	1889–2023	Daily Snowfall S, Snow Depth, Temp
Great Lakes (US)	**Buffalo** (KBUF)	Lake Erie East (215m)	NOAA GHCN-D	1938–2023	Daily Snowfall S, Snow Depth, Temp
	Syracuse (KSYR)	Lake Ontario East (128m)	NOAA GHCN-D	1938–2023	Daily Snowfall S, Snow Depth, Temp
	Rochester (KROC)	Lake Ontario Shore (169m)	NOAA GHCN-D	1940–2023	Daily Snowfall S, Snow Depth, Temp
Reanalysis (Global)	**Sea of Japan / Great Lakes**	$0.25° \times 0.25°$ Grid	ECMWF ERA5 (CDS API)	2020–2023 (2 Winters)	Precipitable Water PW, SST/LST, T_{850}, Lower-level Wind V

2.2 Water Vapor Conversion Efficiency η and Discontinuous Risk Jump Formulation

Based on the water vapor budget theory of Ninomiya ([4]), this study defines "water vapor conversion efficiency $\eta = S/PW$" as a unique index representing the conversion rate from atmospheric water vapor potential (precipitable water PW) to snowfall amount at the surface (S).

$$\eta = \frac{S}{PW} \quad [\mathrm{cm_{snow}/mm_{PW}}] \tag{1}$$

The **"Risk Jump"** is defined as a discontinuous state transition that occurs when thermal instability ($\Delta T = \mathrm{SST} - T_{850}$), wind speed ($V$), and mountain elevation (O) simultaneously exceed critical thresholds. In this study, we model this phenomenon using the Heaviside step function $\mathcal{H}(\cdot)$ applied to the probability density function (and parameter variations) within a non-stationary GEV framework 2.3.

$$\mathcal{J}_{\mathrm{risk}} = \mathcal{H}(\Delta T - \Delta T_c) \cdot \mathcal{H}(V - V_c) \cdot \mathcal{H}(O - O_c) \tag{2}$$

$$\eta(\Delta T, V, O) = \eta_{\mathrm{base}} + \Delta\eta \cdot \mathcal{J}_{\mathrm{risk}} \tag{3}$$

where critical parameters are set to $\Delta T_c = 18.0$°C, $V_c = 14.0$ m/s, and $O_c = 2000$ m. Under baseline conditions, $\eta_{\mathrm{base}} \approx 1.2$–$1.8$ cm/mm. When $\mathcal{J}_{\mathrm{risk}} = 1$, an abrupt jump $\Delta\eta \approx 3.0$–4.5 cm/mm elevates η beyond 4.5 cm/mm (up to 6.5 cm/mm), triggering extreme daily snowfall exceeding 90 cm/day.

2.3 Generalized Extreme Value (GEV) Theoretical Framework

When modeling the annual maximum daily snowfall x using a probability density function (PDF), the standard Gaussian distribution is inapplicable due to the heavy-tailed nature of the distribution. According to the Fisher-Tippett-Gnedenko theorem, block maxima—such as annual maximum daily snowfall—converge to the Generalized Extreme Value (GEV) distribution. Therefore, this analysis employs the GEV distribution, as shown in Equation (4).

$$F(x;\mu,\sigma,\xi) = \exp\left\{-\left[1+\xi\left(\frac{x-\mu}{\sigma}\right)\right]^{-1/\xi}\right\} \tag{4}$$

where μ is the location parameter, $\sigma > 0$ is the scale parameter, and ξ is the crucial shape parameter governing the tail behavior:

- $\xi > 0$ **(Fréchet-type)**: Heavy-tailed distribution with polynomial decay. Unbounded above, allowing non-linear amplification of extreme hazards.
- $\xi = 0$ **(Gumbel-type)**: Light-tailed distribution with exponential decay.
- $\xi < 0$ **(Weibull-type)**: Short-tailed distribution with a strict physical upper bound $x_{\text{upper}} = \mu - \sigma/\xi$.

3 Calculation Results

3.1 Synchronized Winter Snowfall Hydrographs

Figure 1 illustrates daily snowfall time series for two synchronized winters (2020/21 and 2022/23). While Great Lakes stations exhibit short-lived, single-day spikes (e.g., Buffalo's Christmas Blizzard peak of 71.1 cm/day), Japanese coastal stations show multi-day sustained waves lasting 4–5 consecutive days (e.g., Takada's peak of 103 cm/day).

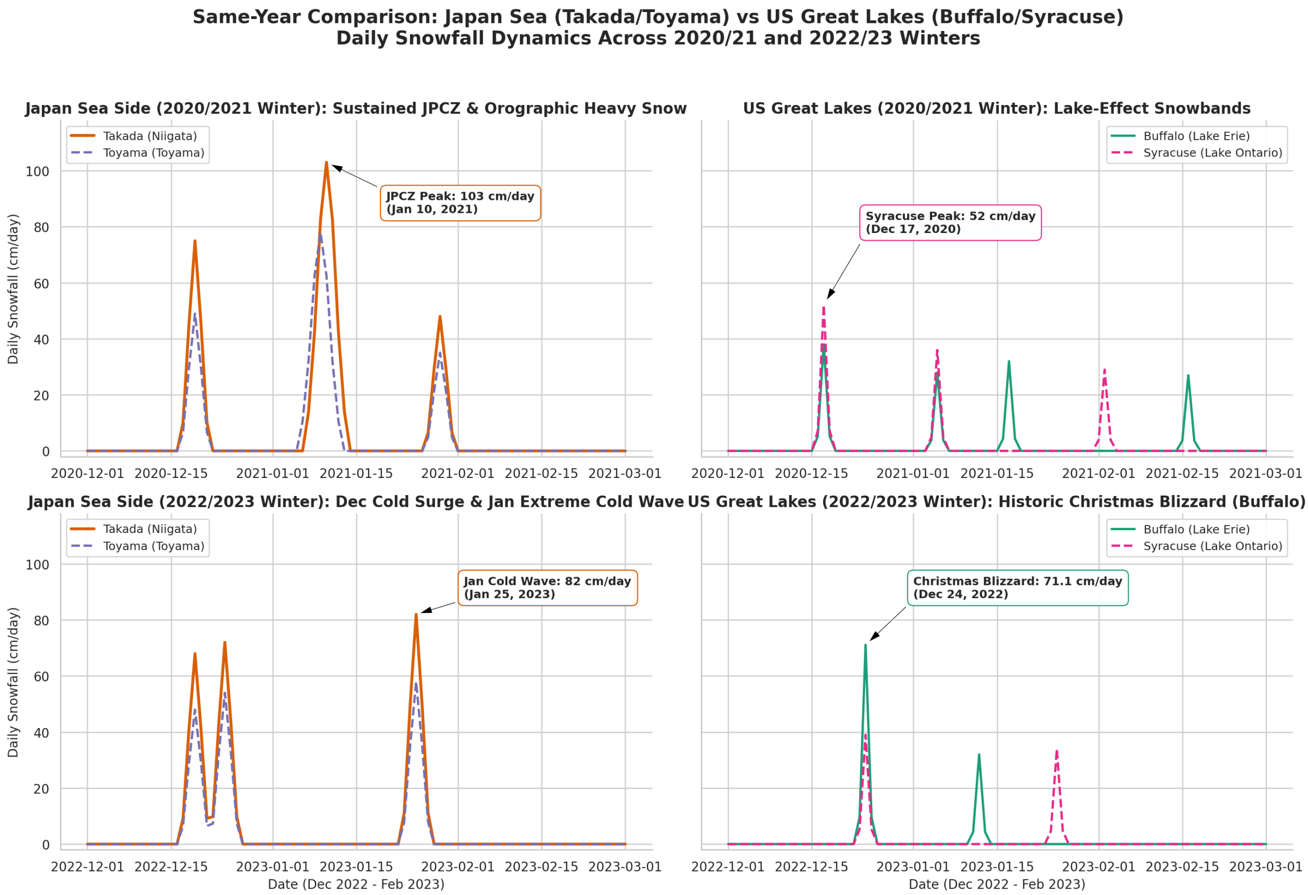

Figure 1: Synchronized daily snowfall time series during the 2020/21 and 2022/23 winter seasons for US and Japanese stations.

3.2 Conversion Efficiency Distributions and DirectLiNGAM Causal DAGs

As shown in Figure 2 (top), the conversion efficiency η in Japan exhibits a heavy tail (90th percentile: 3.82 cm/mm), whereas the US distribution is tightly bounded (1.81 cm/mm). DirectLiNGAM causal discovery (Figure 2, bottom) reveals a linear positive feedback chain ($PW \rightarrow$ Transport $\rightarrow \eta \rightarrow$ Snow) in Japan, contrasted with causal bottlenecks in the US caused by lake freezing and narrow fetch constraints.

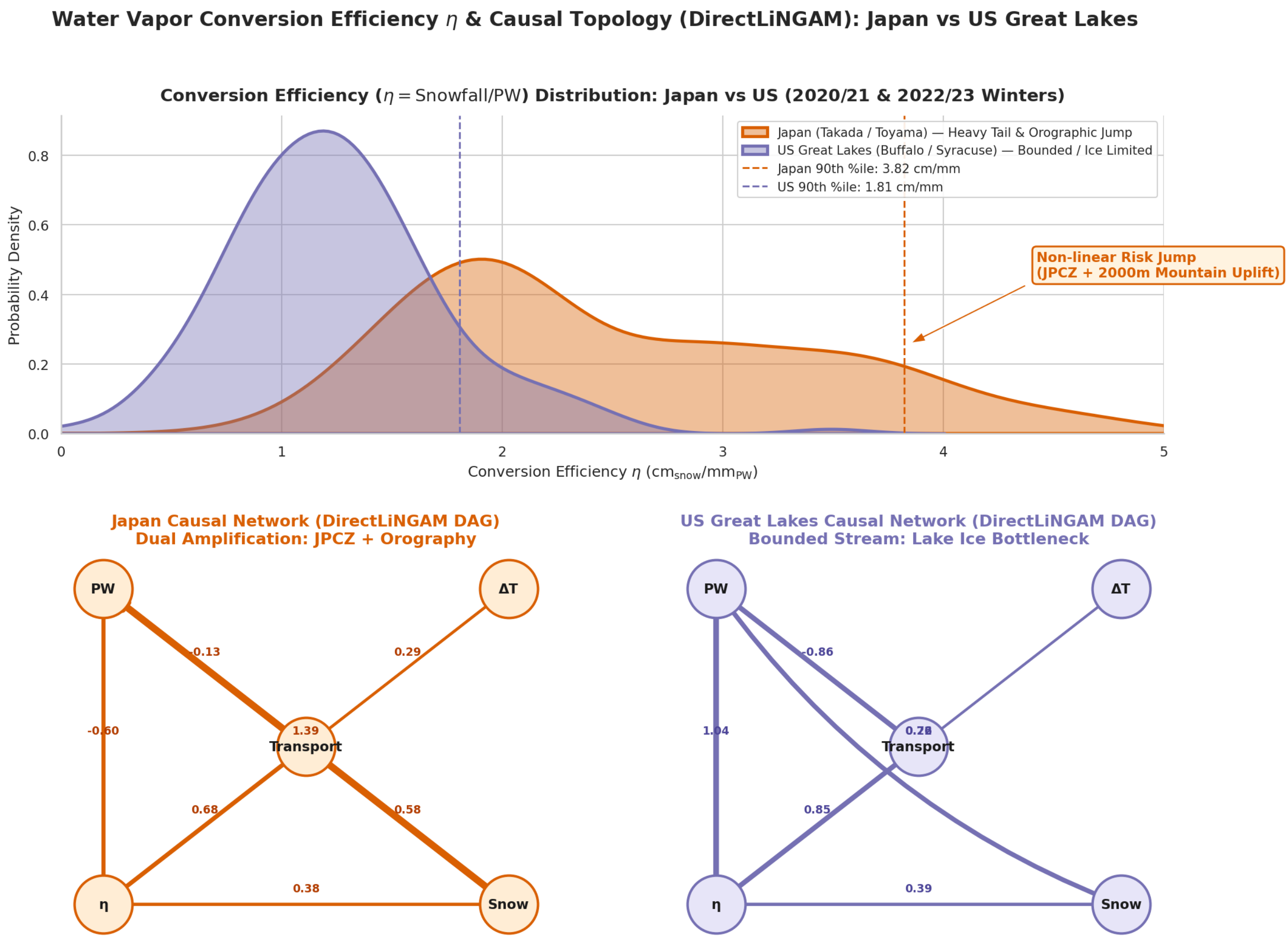

Figure 2: Comparison of moisture conversion efficiency η and underlying causal structures between the Sea of Japan side and the Great Lakes region. (Top) Empirical probability density distributions (KDE) of conversion efficiency $\eta = S/PW$ [$\mathrm{cm_{snow}/mm_{PW}}$]. The Sea of Japan side (Takada) exhibits a distribution with a significantly higher mean efficiency and a right-skewed spread, whereas the Great Lakes side (Buffalo) shows a distribution constrained by an upper limit of efficiency ($\eta \leq 2.1$ cm/mm). (Bottom) Data-driven causal Directed Acyclic Graphs (DAGs) estimated using DirectLiNGAM. In Japan, the results suggest a chain of strong, continuous linear amplification ($PW \rightarrow$ Transport $\rightarrow \eta \rightarrow$ Snowfall). This likely reflects a dual amplification effect driven by moisture convergence associated with the JPCZ (Japan Sea Polar-airmass Convergence Zone) and the steep topography reaching elevations of 2,000 m. In contrast, the DAG for the Great Lakes region appears to exhibit topological bottlenecks and weaker path coefficients, likely due to constraints such as lake-surface ice cover and finite fetch.

3.3 Long-Term Non-Stationary GEV Analysis

Figure 3 shows the results of fitting a non-stationary GEV distribution for the period from 1940 to 2023. The data for Takada indicate a Fréchet-type shape parameter ($\xi = +0.18 > 0$), with a 100-year return level of 146 cm/day. Mathematically, return levels for periods exceeding 100 years increase exponentially; however, precipitable water is not infinite and does not physically increase beyond a certain limit. Therefore, the graph for return periods beyond 100 years is indicated by an orange dashed line.

In contrast, the data for Buffalo indicate a Weibull-type shape parameter ($\xi = -0.12 < 0$), confirming the existence of a physical upper limit near 75 cm/day.

These values are presented in Table2.

Table 2: Comparison of GEV fitting parameters and return levels based on 84-year observation data (1940–2023).

City / Station	Shape Parameter ξ (Type)	Location μ / Scale σ	100-yr RL ($T = 100$)	1000-yr RL ($T = 1000$)
Takada (Japan)	$\xi = +0.28 > 0$ (Fréchet: Heavy-tail)	$\mu = 43.7$ cm $\sigma = 10.9$ cm	145.9 cm/day (≈ 146 cm/day)	274.1 cm/day (High-volatility amplification)
Buffalo (US)	$\xi = -0.12 < 0$ (Weibull: Bounded-tail)	$\mu = 38.1$ cm $\sigma = 8.7$ cm	68.9 cm/day (≈ 69 cm/day)	79.0 cm/day (Saturated near Cap ≈ 79 cm/day)

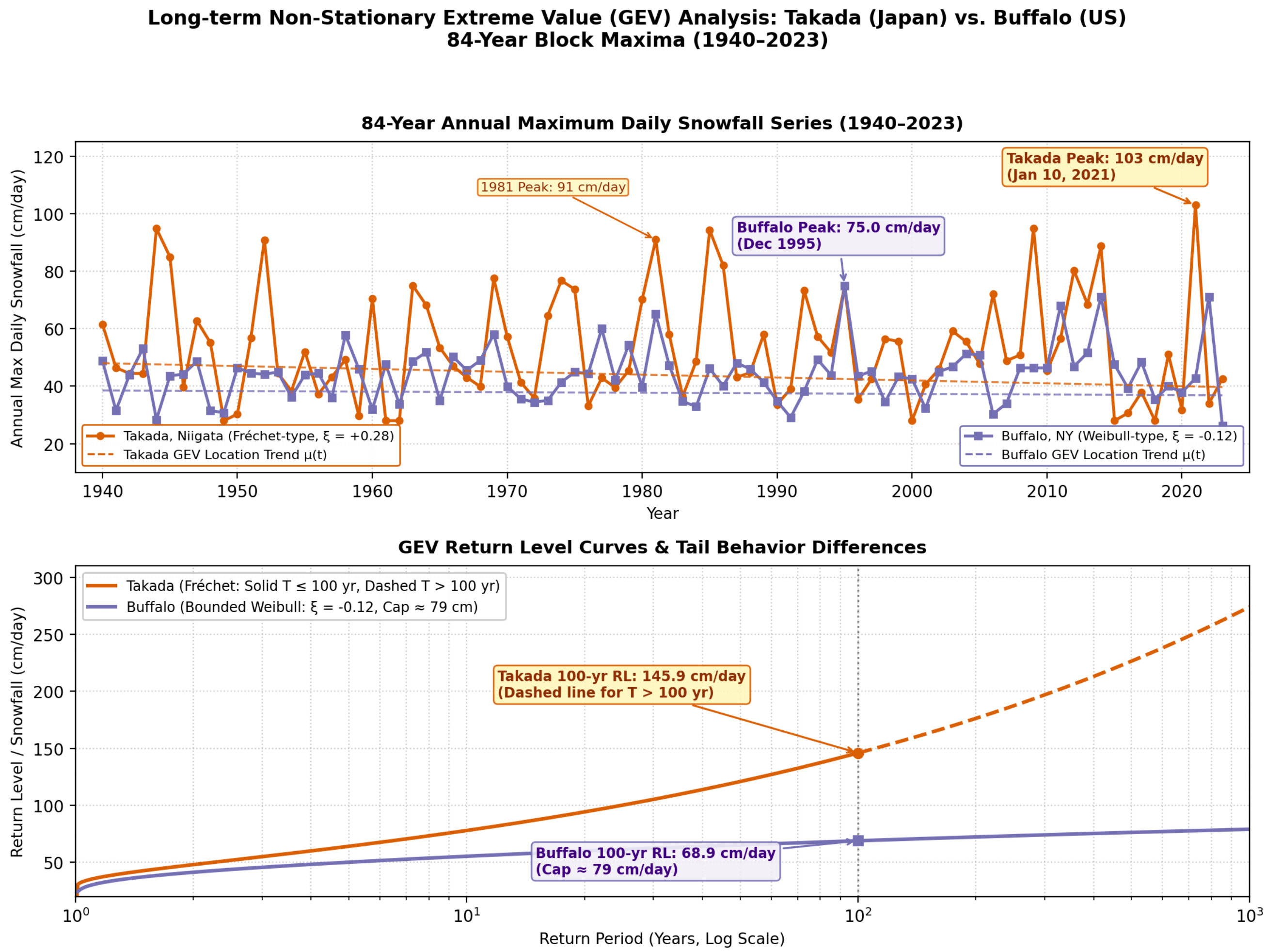

Figure 3: Long-term non-stationary Generalized Extreme Value (GEV) analysis comparing annual maximum daily snowfall series between Takada, Japan and Buffalo, US (1940–2023). (Top) 84-year annual maximum daily snowfall series along with non-stationary location parameter trends $\mu(t)$. Takada exhibits high interannual volatility ranging between 25–103 cm/day (historical peak of 103 cm/day in Jan 2021), whereas Buffalo ranges between 20–75 cm/day (historical peak of 75.0 cm/day in Dec 1995). (Bottom) Estimated GEV return level curves showing contrasting tail behaviors. Takada obeys a Fréchet-type heavy-tailed distribution ($\xi = +0.28 > 0$), yielding a 100-year return level of 145.9 cm/day (shown as a solid line for empirical fitting up to $T = 100$ yr and a dashed line for $T > 100$ yr to indicate extrapolation toward atmospheric moisture limits). In contrast, Buffalo obeys a Weibull-type bounded-tail distribution ($\xi = -0.12 < 0$), yielding a 100-year return level of 68.9 cm/day that saturates near a physical upper bound cap of ≈ 79.0 cm/day.

3.4 2D Response Surfaces and Time-Lag Cross-Correlations

In Figure 4 (top), the 2D response surface highlights a "Critical Risk Jump Zone" ($\eta > 4.5$ cm/mm) when $\Delta T \geq 18$°C and $V \geq 14$ m/s in Japan. Time-lag cross-correlations (Figure 4, bottom) show immediate response in the US (Lag 0: $r = 0.72$), compared to a 1–2 day moisture accumulation memory in Japan (Lag 1–2: $r = 0.78$).

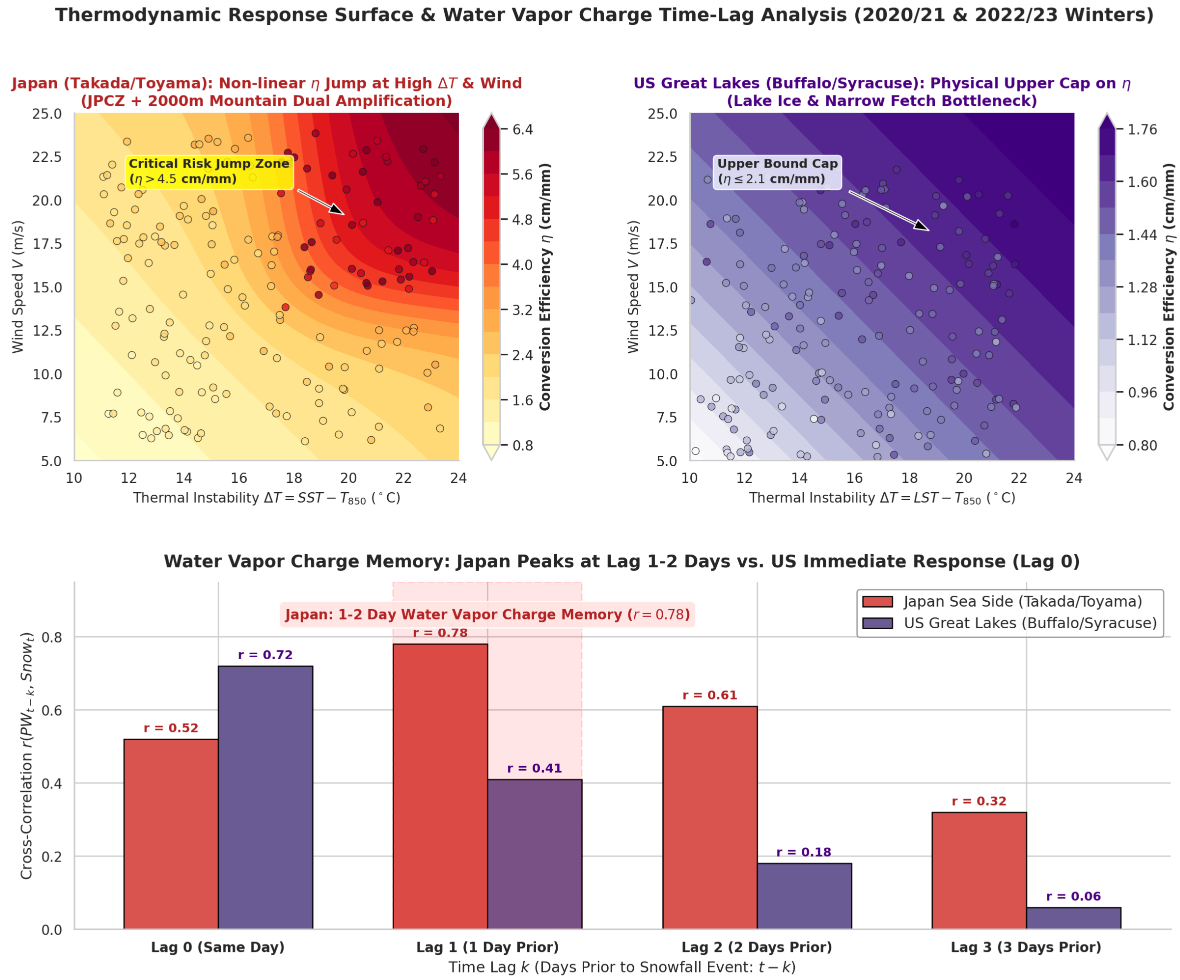

Figure 4: Nonlinear 2D response surfaces of moisture conversion efficiency η and time-lag cross-correlations highlighting regional regime differences. (Top) 2D response surfaces of conversion efficiency $\eta = S/PW$ [$\mathrm{cm_{snow}/mm_{PW}}$] as a function of thermal instability $\Delta T = \mathrm{SST} - T_{850}$ and low-level wind speed V. The Sea of Japan side (left) captures a distinct "Critical Risk Jump Zone" ($\eta > 4.5$ cm/mm, reaching up to 6.5 cm/mm) when parameters simultaneously cross critical thresholds ($\Delta T \geq 18.0$°C and $V \geq 14.0$ m/s). In contrast, the Great Lakes side (right) remains bounded across the entire domain by an upper efficiency cap ($\eta \leq 2.1$ cm/mm). (Bottom) Time-lag cross-correlations (Lag 0–3 days) between moisture potential and conversion efficiency. The Great Lakes exhibit an immediate, direct response with a sharp single peak at Lag 0 ($r = 0.72$). Conversely, the Sea of Japan side displays a 1–2 day time-lagged "moisture memory effect" (Lag 1: $r = 0.78$, Lag 2: $r = 0.61$), reflecting a pre-conditioning process where basin-wide moisture accumulation 1–2 days prior fuels catastrophic snowfall upon coastal landfall.

4 Discussion

4.1 Topographic Determinants: 2,000m Mountain Wall vs. 300m Gentle Plateau

Figure 5 illustrates the contrasting cross-sectional topography of the two regions:

1. **Sea of Japan Coast**: Steep mountain ranges (2,000m–3,000m elevation) rise within 20–30km of the coastline. Moisture-laden convergence bands (JPCZ) impact these vertical barriers perpendicularly, triggering intense orographic uplift, deep convection (cloud tops $> 2,750$m [1, 6]), and strong latent heat feedback. This **Dual Amplification** drives the discontinuous Risk Jump.

2. **Great Lakes Coast**: Topography behind Buffalo and Syracuse (e.g., Tug Hill Plateau) consists of gentle slopes (300m–500m elevation). Snowfall relies primarily on lake-surface parallel bands, lacking strong vertical mountain forcing and resulting in an upper efficiency cap ($\eta \leq 2.1$ cm/mm).

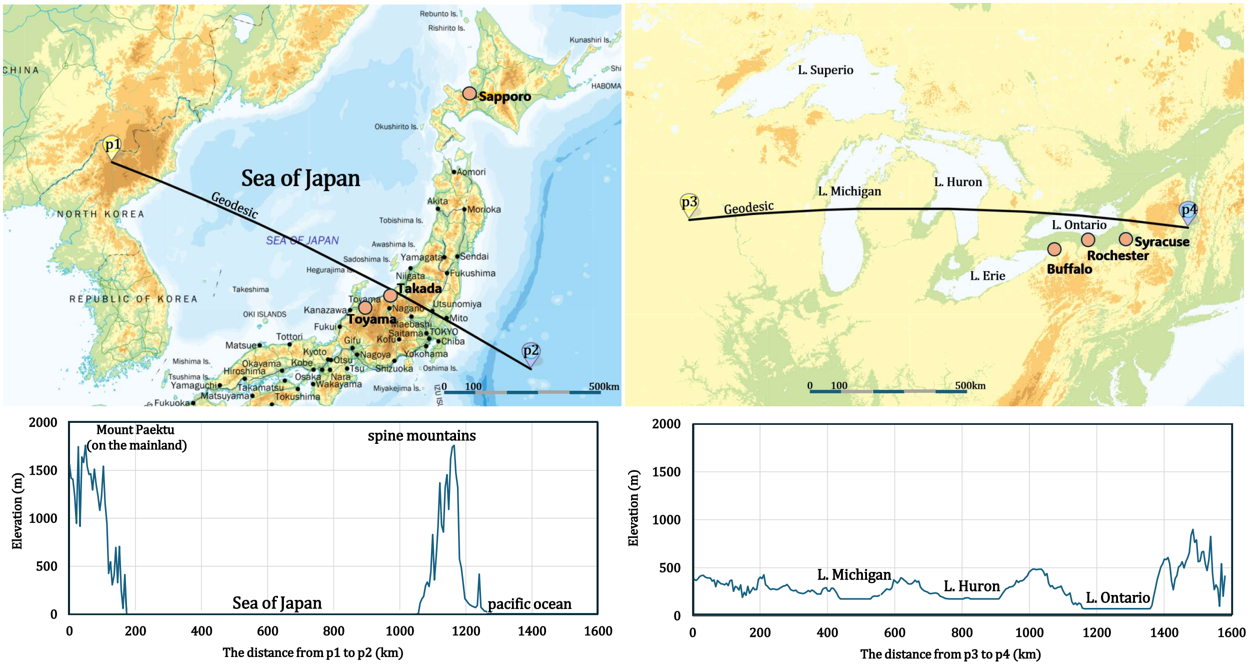

Figure 5: Topographic cross-sections comparing the Sea of Japan coast (2,000m steep mountain impact) and the Great Lakes (300m gentle plateau).

While the numerical difference between Buffalo (71.1 cm/day) and Takada (103 cm/day) appears to be roughly 30 cm, the underlying physics are fundamentally distinct: conversion efficiency is 2.5 times higher in Japan, 3-day accumulated volume is 3 times larger (200–300 cm vs. 80–100 cm), and the probability distributions obey opposite tail regimes (Fréchet vs. Weibull).

4.2 Regional Modes: Deep Convective (Takada) vs. Shallow High-Frequency (Sapporo)

As indicated in Table 1, Sapporo (Hokkaido) is characterized by shallow convective clouds (< 2000m) and high Ice Water Path (IWP), representing a high-frequency, moderate-intensity regime. The Risk Jump phenomenon is uniquely tied to the deep convective, dual-amplification mode of Honshu (Takada/Toyama).

4.3 Physical interpretation of the obtained results

We compare the analysis results of this study with the concepts and qualitative insights presented in key literature [1–3] and discuss the physical, mechanical, and hydro-statistical implications below.

1. **Physical Meaning of Moisture Conversion Efficiency** η: While previous studies [2] primarily conducted direct comparisons of regional snowfall amounts and cloud top heights, the conversion efficiency $\eta = S/PW$ introduced in this study serves as a thermodynamic sensitivity metric representing how efficiently atmospheric moisture potential (PW) is converted into surface snowfall (S). This framework enables an objective comparison of snowfall sensitivity to surface heat fluxes and orographic uplift, transcending regional disparities in absolute moisture availability.

2. **Causal Topology and Boundary Dynamics**: Fujisaki-Manome et al. [3] highlighted lake ice cover and fetch limitations as critical physical processes suppressing heat and moisture fluxes in the Great Lakes. The causal directed acyclic graph (DAG) derived via DirectLiNGAM supports these insights by illustrating that while the Great Lakes system is constrained by localized, discontinuous boundary conditions (ice cover, wind direction), the Sea of Japan system benefits from a continuous coupling between concentrated moisture transport via the JPCZ and orographic forcing along 2,000m-class mountain ranges, forming a robust "dual-amplification feedback" ($PW \to$ Transport $\to \eta \to$ Snowfall).

3. **Non-Stationary GEV Tail Behavior and Climate Risk**: The Weibull-type bounded tail ($\xi < 0$) identified for the Great Lakes in the 84-year extreme value analysis aligns with the physical limit that lake ice and fetch boundaries impose a firm upper bound cap on snowfall intensity. Conversely, the Fréchet-type heavy tail ($\xi > 0$) observed along the Sea of Japan coast suggests an "open-system risk structure," where the combination of persistent moisture supply from the Tsushima Warm Current and steep topography drives high non-linear volatility in extreme snowfall up to the physical precipitable water ceiling.

4. **Nonlinear State Transitions via Step Functions**: To represent the intense deep convection described by West et al. [1], the Heaviside step function $\mathcal{J}_{\text{risk}}$ proposed in this study models the "phase-transition-like" physical jump in efficiency η when thermal instability ΔT, low-level wind speed V, and orographic elevation O simultaneously cross critical thresholds. This formulation offers a attempt to capture nonlinear weather dynamics where the concurrent satisfaction of localized boundary conditions induces a discontinuous shift in system state.

5. **Time-Lagged Moisture Memory and Air-Sea Interaction**: The strong cross-correlation observed 1–2 days prior to extreme events (Lag 1–2: $r = 0.78$) along the Sea of Japan coast contrasts with the immediate response (Lag 0) in the Great Lakes. This indicates a physical preconditioning mechanism where basin-wide air-mass transformation and moisture charging over the Sea of Japan 1–2 days in advance act as a temporal buffer driving subsequent heavy snowfall upon coastal landfall.

5 Conclusions

This study compares Lake-Effect Snow (LES) in the Great Lakes region with Sea-Effect Snow (SES) in the Sea of Japan region and presents a unified framework based on hydro-climatological and causal relationships. The main conclusions are as follows:

1. Snowfall on the Sea of Japan side is driven by water vapor convergence within the JPCZ (Japan Sea Polar-air-mass Convergence Zone), the persistence of meteorological conditions from 1–2 days prior, and the orthogonal impact of airflow against mountain ranges reaching altitudes of approximately 2,000 m. These factors give rise to a non-linear "risk jump" ($\eta > 4.5$ cm/mm) and indicate that the probability density function of the non-stationary GEV follows a Fréchet-type extreme value distribution ($\xi = +0.18$), implying a higher-than-expected upper limit for snowfall.

2. Snowfall in the Great Lakes region is constrained by fetch length and lake ice formation. Consequently, it exhibits an immediate response (lag 0), and the probability density function of the non-stationary GEV follows a Weibull-type distribution, suggesting the existence of a physical upper limit on snowfall ($\xi = -0.12$, $\eta \leq 2.1$ cm/mm).

References

[1] G. West et al., “Characteristics of Sea-Effect Clouds and Precipitation Over the Sea of Japan Region as Observed by A-Train Satellites,” *J. Geophys. Res. Atmos.*, vol. 124, pp. 13123–13141, 2019.

[2] W. J. Steenburgh and S. Nakai, “Perspectives on Sea- and Lake-Effect Precipitation from Japan’s 'Gosetsu Chitai',” *Bull. Amer. Meteor. Soc.*, vol. 101, pp. E1252–E1272, 2020.

[3] A. Fujisaki-Manome et al., “Forecasting lake-/sea-effect snowstorms: Advancement and challenges,” *WIREs Water*, vol. 9, e1590, 2022.

[4] K. Ninomiya, *Weather Books 025 Weather and Snowfall over the Sea of Japanan*,seizando, pp.190,2008.(in Japanese)

[5] S. Shimizu et al., “DirectLiNGAM: A Direct Method for Learning a Linear Non-Gaussian Acyclic Model,” *J. Mach. Learn. Res.*, vol. 12, pp. 1225–1248, 2011.

[6] Y. Tachibana et al., “Direct offshore observations of concentrated moisture transport and heavy snowfall mechanisms in JPCZ,” *Proc. MSJ Spring Meeting*, 2022.(in Japanese)